Strong Ground Motion Simulation for the 2005 Fukuoka Earthquake (Mw6.6) by Stochastic Finite-Fault Simulations

MITSUTAKA OSHIMA[1], HIROSHI TAKENAKA[1], and HIROSHI KAWASE[2]

[1] Dept. of Earth and Planetary Sciences, Kyushu University,6-10-1 Hakozaki, Fukuoka, Japan
[2]Disaster Prevention Research Institute, Kyoto University, Gokasho, Uji, Kyoto, Japan
Email: kouki@geo.kyushu-u.ac.jp, takenaka@geo.kyushu-u.ac.jp, kawase@zeisei.dpri.kyoto-u.ac.jp

ABSTRACT :
The theoretical basis of the stochastic finite-fault modeling was proposed by Boore (1983) and this technique has been developed by many researchers (g.e., Beresnev and Atkinson, 1997) and many papers were published applying it to real simulations. Recently, Motazedian and Atkinson (2005) have introduced the concept of "dynamic corner frequency" and "pulsing area" into the stochastic finite-fault modeling. It is possible to simulate strong ground motions from earthquakes in a more realistic way with these new concepts. We made a further modification that enables us to treat stress parameter variable on the fault plane, while the stress parameter is constant on the whole fault plane in the conventional stochastic finite-fault modeling. With this modification, we can introduce stress-variable source models such as asperity model. We apply our modified stochastic finite-fault modeling to the 2005 West Off Fukuoka earthquake (Mw6.6) that occurred in northwest Kyushu, Japan, and check whether we could satisfactorily reproduce the observed strong ground motion data. We adopt an asperity model and assign higher stress parameter to the asperity than that of the background region. To incorporate accurate site amplification effects, we employ site amplification data extracted by Kawase and Matsuo (2004) using the spectral separation technique. The obtained synthetic Fourier amplitude spectra and time series show overall agreement with the observed ones. In particular, the agreement of the Fourier amplitude spectra are quite well.

KEYWORDS:
Strong Ground Motion Simulation, Stochastic Finite-Fault Simulation, 2005 West Off Fukuoka Earthquake

1. INTRODUCTION

Strong ground motion simulations based on asperity models have been eagerly executed in the world. The asperity was defined by Somerville et al. (1999) as the region that has the slip twice as large as the slip averaged on the whole fault plane and was reported that they accounts for approximately 22 % of the whole fault area. Asperity models are simplified source models and expressed by a few parameters. With the asperity models, we can simulate future earthquakes without setting too many complex parameters and obtain results with certain validity. In this paper, we incorporate asperity model in the stochastic finite-fault modeling. In strong ground motion simulation based on the asperity models, we have to set two stress parameters: one is for asperity region and the other is for the rest portion of the fault plane. In general, determination of unknown parameters needs many calculations and the increase of unknown parameters should be avoided. Besides this, the setting of unknown parameters maybe arbitrary and dependent on researchers. To avoid such situations, we exploit a new approach that uses empirical relation between the seismic moment and the high-frequency level of source spectrum shown by Dan et al. (2001) to confine stress parameters. The only unknown input parameter in our simulation is the ratio between stress parameter at asperity region and that at the rest.

We use the code of Beresnev and Atkinson (1998a) after modification to incorporate the new concepts of "dynamic corner frequency" and "pulsing area" proposed by Motazedian and Atkinson (2005). About the detailed information on the two concepts, please see Motazedian and Atkinson (2005). We also develop a new way to determine the "pulsing area" objectively and uniquely by forcing radiated energy from all subfaults to equal to "reference energy", which is described in the following section. In our approach, the "pulsing area" is automatically determined, where it has been determined by a trial and error fashion, so far. In determination of "pulsing area", we take into consideration the random summation of energy radiated from subfaults.

We also incorporate frequency dependent radiation coefficients. The frequency dependent behavior of

radiation coefficients was reported by some researchers (e.g., Takenaka et al., 2002), where conventional stochastic finite-fault modeling uses azimuthal root-means-squares average of the radiation coefficients, namely, radiation coefficient is assumed to be isotropic at all frequencies. Generally, radiation coefficients become isotropic at high frequencies and shows double-couple type pattern at low frequencies. To incorporate this effect, we adopt the method proposed by Kagawa (2004).

Finally, we simulate the strong ground motion of the 2005 West Off Fukuoka Earthquake by adopting asperity model and our new approach to check whether our new method work well.

2. METHOD

Here, we mainly show how we determined the stress parameter for asperity model and how we set the pulsing area. We also refer to the frequency dependent radiation coefficients used in our study.

2.1. Determination of Stress Parameter for Asperity Model

In simulation based on asperity models, we have to set two stress parameters: one is for asperity region and the other is for the rest. We determine them assuming that the sum of the high-frequency level of the acceleration source spectrum of asperity region and that of the rest region equals the high-frequency level of source spectrum expected from seismic moment through an empirical relation between seismic moment and high-frequency level of source spectrum shown by Dan et al. (2001).

According to Irikura et al. (2004), the high-frequency level of the acceleration source spectrum from asperity is expressed as following, with reference to Madariaga (1977) and Boatwright (1988).

$$A_a = 4\sqrt{\pi}\beta v_r \sqrt{S_a}\Delta\sigma_a \quad , \tag{2.1}$$

where A_a is the high-frequency level of acceleration source spectrum of asperity region, β is shear wave velocity, v_r is rupture velocity, S_a is the area of asperity region, and $\Delta\sigma_a$ is the stress parameter at asperity region. We assume the same form for high-frequency level of the rest region as following,

$$A_b = 4\sqrt{\pi}\beta v_r \sqrt{S_b}\Delta\sigma_b \quad . \tag{2.2}$$

Subscripts “a” and “b” specify asperity region and the rest region, respectively. Here we assume that all subfaults are of the same area: S_e, and asperity region and the rest region are comprised of n_a subfaults and n_b subfaults, respectively. Then the sum of the high-frequency level of asperity region and the rest, we refer as A, is shown as

$$A = \left\{16\pi\beta^2 v_r^2 S_e (n_a \Delta\sigma_a^2 + n_b \Delta\sigma_b^2)\right\}^{1/2} \quad . \tag{2.3}$$

We assumed $A = \sqrt{A_a^2 + A_b^2}$, taking into consideration the sum of the randomly distributed energy.

On the other hand, Dan et al. (2001) showed an empirical relation between seismic moment and high-frequency level of acceleration source spectrum as

$$A = 2.46\times10^{17} \times M_0^{1/3} \quad , \tag{2.4}$$

where A is high-frequency level of acceleration source spectrum in dyne-cm/s^2, M_0 is seismic moment in dyne-cm. We introduce the ratio of two stress parameters at asperity region and the rest region: R_{ab} and express $\Delta\sigma_a$ as

$$\Delta\sigma_a = R_{ab}\Delta\sigma_b \quad , \tag{2.5}$$

then substitute this to equation (2.3). Then equating equation (2.3) and (2.4) we obtain equation about R_{ab} and $\Delta\sigma_b$. Once we specify R_{ab} then we can automatically determine $\Delta\sigma_b$ and $\Delta\sigma_a$ is also automatically determined through equation (2.5).

In our approach, as shown above, the only parameter we have to specify when we do stochastic finite-fault modeling based on asperity models is R_{ab} and we can reduce arbitrariness in determination of stress parameters for asperity region and the rest region.

2.2. Determination of Pulsing Area

Pulsing area is the concept introduced into stochastic finite-fault modeling by Motazediana and Atkinson (2005) and this parameter determines the actually rupturing area at the specified time. This parameter controls

the way in which energy from subfaults is radiated through dynamic corner frequency, especially at low frequency level of source spectrum, and the value of this parameter has been determined in trial and error fashion. We determine this parameter more objectively and automatically by introducing "reference energy" and equating this with total energy radiated from all subfaults. Namely, we put an energy conservation constraint on the pulsing area and therefore the total radiated energy from all subfaults must be always equal to the reference energy.

We introduce reference energy: E_{ref} shown by

$$E_{ref} = \int \{CM_0 (2\pi f)^2 / [1+(f / f_0)^2]\} df \ , \tag{2.6}$$

where M_0 is seismic moment, f is frequency, f_0 is the corner frequency, and $C = R^{\theta\phi} FV / (4\pi\rho\beta^3)$, where $R^{\theta\phi}$ is radiation pattern, F is amplification at free surface, V is partition onto two horizontal directions, ρ is density, and β is shear wave velocity. Total energy from all subfaults: E_{total} is expressed as

$$E_{total} = correction \times \sum_{i=1}^{nl} \sum_{j=1}^{nw} \int \{CM_{ij} (2\pi f)^2 / [1+(f / f_{0ij})^2]\} df \ , \tag{2.7}$$

where nl is the number of subfaults in length direction, nw is the number of subfaults in width direction, M_{ij} is seismic moment of the ijth subfault on the fault plane, and f_{0ij} is the corner frequency of the ijth subfault. $correction$ is the correction factor to take into account the summation of randomly distributed energy. To a first approximation, we define $correction$ as

$$correction = \left(\frac{\sqrt{dl \cdot dw / \pi}}{v_r \cdot nl \cdot nw \cdot dur} \right)^{1/2} \ , \tag{2.8}$$

where dl is length of subfault, dw is width of subfault, and dur is duration of synthetic waveform defined below equation.

$$dur = d\max 1 + d\max 2 - d\min 1 \tag{2.9}$$

Here, $d\max 1 = \max_{i,j} \left(r_{ij} / v_r + R_{ij} / \beta \right)$, $d\min 1 = \min_{i,j} \left(r_{ij} / v_r + R_{ij} / \beta \right)$, and $d\max 2 = \max_{i,j} \left(duration(R_{ij}) \right)$, where r_{ij} is the distance from the rupture initiation point to the ijth subfault, R_{ij} is the distance between the ijth subfault and the observation point, and $duration$ is the duration time that defined by duration models according to R_{ij}.

By equating equation (2.6) and (2.7), we can automatically and uniquely determine the pulsing area. We need not to do many calculations to determine pulsing area any more with this approach.

2.3. Frequency Dependent Radiation Coefficient

In conventional stochastic finite-fault modeling, radiation coefficients are kept constant in all directions. This is valid for high frequencies but radiation coefficients shows deterministic behavior at low frequencies. In this study, we use the frequency dependent radiation coefficients model proposed by Kagawa (2004):

$$R_{\theta\phi}(f) = \frac{(\log(f_2) - \log(f)) R_{\theta\phi 0} + (\log(f) - \log(f_1)) R_{\theta\phi m}}{\log(f_2) - \log(f_1)} \ , \tag{2.10}$$

where $R_{\theta\phi 0}$ is theoretical radiation coefficients determined by relative locations of observation point and source and slip direction, $R_{\theta\phi m}$ is isotropic stochastic radiation coefficients at high frequency, and f_1 and f_2 are frequency that defines the transition range between theoretical and isotropic radiation coefficients.

3. DATA

We use acceleration records of K-NET and KiK-net stations of NIED (National Research Institute for Earth Science and Disaster Prevention). We use strong motion data of 25 stations and all those stations are depicted in Fig.1.

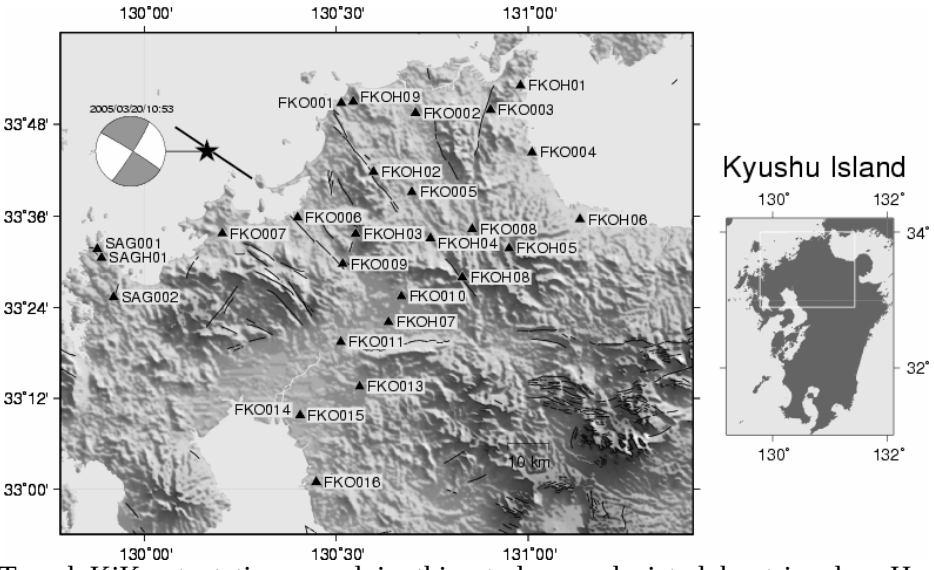

Figure.1 K-NET and KiK-net stations used in this study are depicted by triangles. Hypocenter of the mainshock of the 2005 West Off Fukuoka Earthquake is also depicted as star with the mechanism. Black solid lines stand for active faults (The Research Group for Active Faults of Japan, 1991). The rectangular region outlined by white solid lines of the map in the right hand side shows the region illustrated in the left hand side map.

Hypocentral distances of the stations range from 22 km to 92 km. All of the acceleration data we used in this study is corrected for the orientation of seismometers. Then all acceleration data is band-pass filtered 1-10 Hz after the correction for baseline. Observed waveforms at 25 stations we use in the simulation are shown in Fig.3.

4. ANALYSIS

We execute stochastic finite-fault modeling with above shown new approaches to reproduce strong ground motion of the 2005 West Off Fukuoka Earthquake. We set asperity region in view of the slip distribution obtained by waveform inversion (e.g. Asano and Iwata, 2006, Kobayashi et al., 2006). The slip weight assigned to asperity region and the rest region is seven and three, respectively. Those weights are determined so that the slip at asperity region is to be twice as large as that averaged on the whole fault plane. We do not use f_{max} filter because we can not find out any sign of f_{max} effect at frequency range between 1 Hz to 10 Hz. To incorporate anelastic attenuation, we use frequency dependent quality factor that was obtained by Takenaka and Mamada (2004) for the target region of this study. About all stations use in this study, site amplification effects of all the stations were extracted by Kawase and Matsuo (2004a,b) from ground motion data including aftershocks of West Off Fukuoka Earthquake, using spectral separation technique. We use their site amplification data to take into account the amplification effects below each station precisely. We also set the transition frequency that controls the behavior of frequency dependent radiation coefficient as 1.0 Hz and 2.0 Hz, because Takenaka et al. (2003) found that radiation coefficients nearby our target region become isotropic above 2.0 Hz.

We show input parameters used in our simulation in Table.1. The fault geometry is also illustrated in Fig.2. Since the only unknown input parameter necessary for our simulation is the ratio between stress parameter at asperity region and the rest region, we do simulation by changing the ratio between stress parameter at asperity region and that at the rest region. Then we visually compare the synthetic waveforms and Fourier amplitude spectra of them with those for observed data and determined the stress ratio that gives the best matching between synthetics and observed data.

Pulsing area and stress parameters at asperity and the rest regions are determined automatically by using our new approach.

Table.1 Input modeling parameters.

Parameter	Value
Fault orientation (strike/dip)	304/87
Fault dimension along strike and dip (km)	24 x 18
Subfault size	2 km x 2 km
Depth of the upper edge of the fault (km)	1
Main shock moment magnitude	6.6
Nucleation subfault (number along strike and dip)	(5,5)
Crustal shear wave velocity (km/s)	3.46
Crustal density (g/cm^3)	2.7
Attenuation model	$Q(f)=97f^{0.59}$

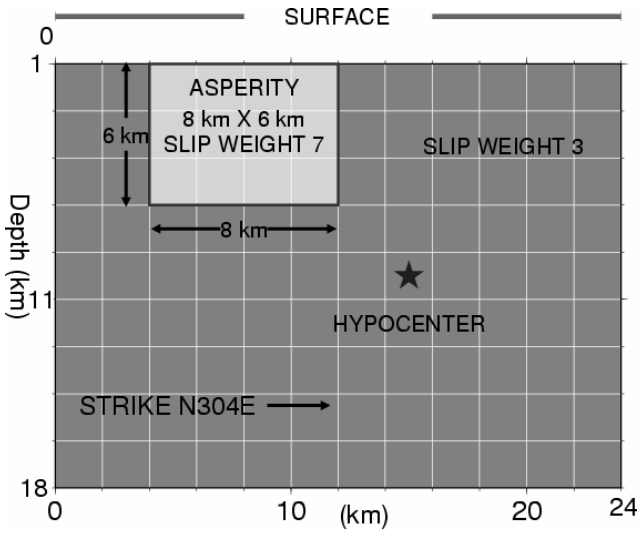

Figure.2 Fault geometry used for simulation. Fault size is 24 km in length direction and 18 km in depth direction. Each square outlined by white solid lines shows subfault. Fault plane was divided into 12 x 9 subfaults. White colored rectangular signifies asperity region at which slip weight is seven. The rest area has slip weight of three. Hypocenter is illustrated by black star.

5. RESULTS

The ratio between asperity region and the rest region that gives the best match between the synthetic and observed data was 2. The resultant stress parameter at asperity region was about 200 bar and the stress parameter at the rest region was 100 bar. We show observed waveforms and resultant synthetic waveforms in Fig.3. Visually comparing the synthetic waveforms and observed waveforms they resembles well except station KF06, KF07, KF09, and KF14, where synthetic waveforms are overestimated compared to the observed waveforms, even at stations that have small hypocentral distance, e.g. KF01 and KF07. Fourier amplitude spectra of observed data and synthetics are plotted in Fig.4. Fourier spectra of synthetics and observed matches well, especially in shape. The matching of synthetics and observed data seems good. We also show spectral ratio of Fourier amplitude spectra of observed data and synthetics averaged over all stations in Fig.5. This figure shows our results are satisfactory in average, although there are deviation from unit at some frequencies (e.g. around 0.7 Hz).

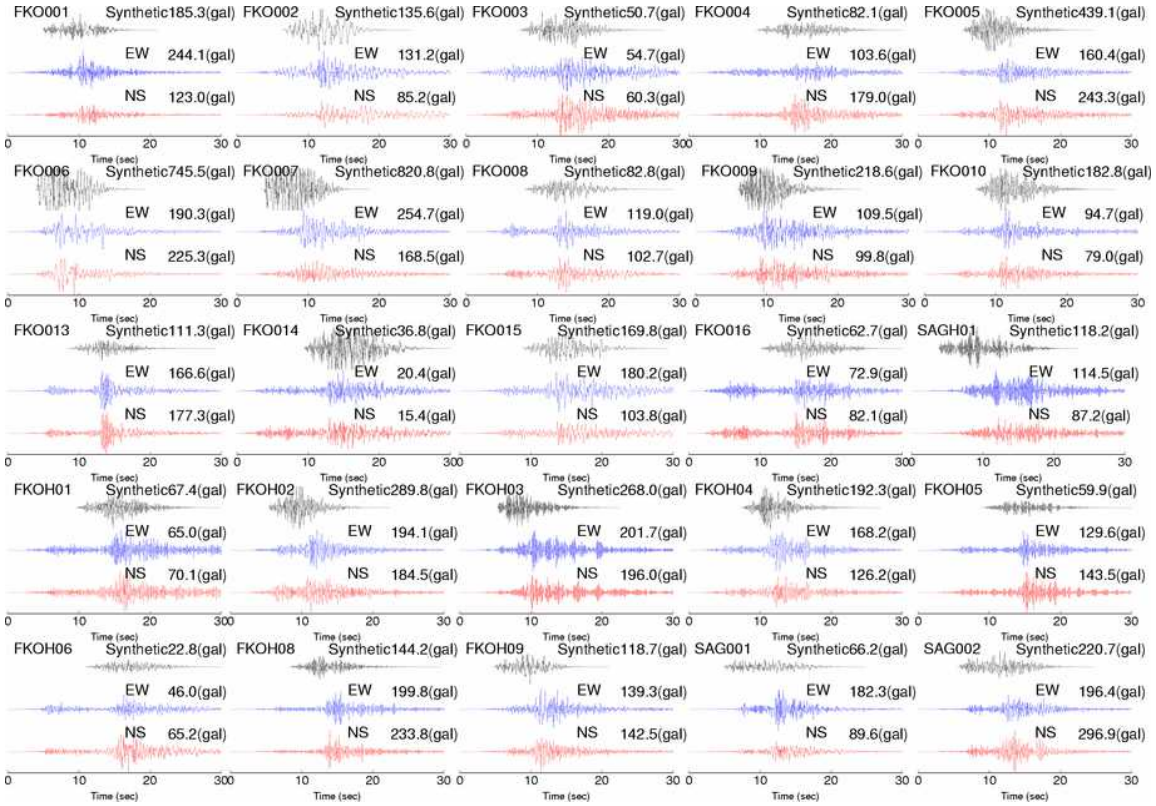

Figure.3 Synthetic and observed waveforms. Lowermost traces are the north-south component of the observed waveforms. The middle traces are the east-west component of the observed waveforms. The uppermost traces are synthetics waveforms. The maximum amplitude of each trace is attached in the upper left in gal.

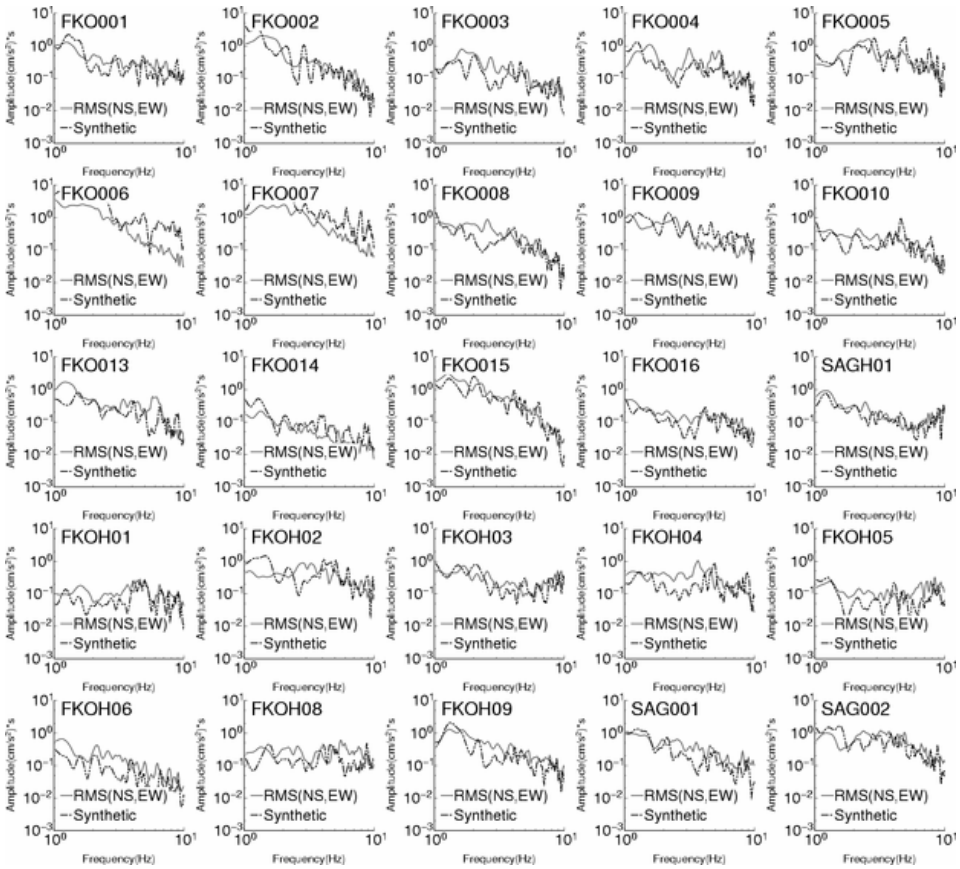

Figure.4 Acceleration Fourier amplitude spectra of synthetics and observed data are shown. Solid black lines stand for the root mean square averaged Fourier amplitude spectra of north-south and east-west component of observed data. Solid green lines signify the Fourier amplitude spectra of synthetics.

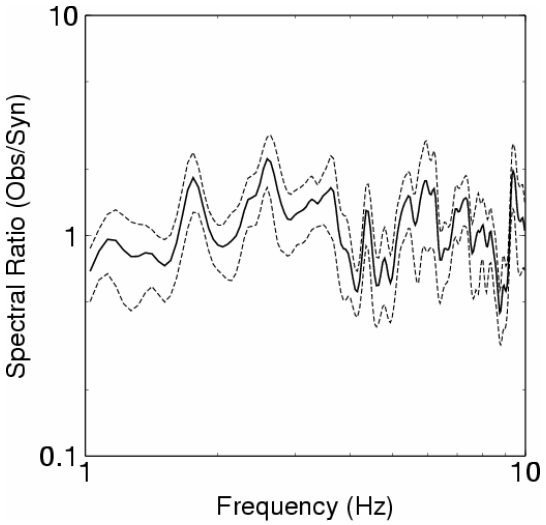

Figure.5 Average ratio of Synthetic and observed Fourier amplitude spectra is illustrated against frequency. Axes are both logarithmic. Average spectral ratio is plotted with solid bold line and the 95% confidence level of the average is depicted with thin dashed lines.

6. DISCUSSION AND CONCLUSIONS

We could reproduce strong ground motion of the 2005 West Off Fukuoka Earthquake both in time and frequency domain as a whole.

We developed a new approach to incorporate asperity models into stochastic finite-fault modeling and to determine stress parameters both for asperity region and the rest region using empirical relation between seismic moment and high frequency acceleration source spectrum by Dan et al. (2001). By using this new approach, it became possible to incorporate asperity models into stochastic finite-fault modeling and to determine stress parameters for both asperity region and the rest region by just specifying the ratio between the stress parameter at the two regions. So we can do stochastic finite-fault modeling incorporating asperity models without any increase in the number of unknown input parameters.

We also presented a new way to determine pulsing area by introducing energy conservation constraint. Our new way enables us to determine pulsing area objectively and uniquely, although the pulsing area has been determined in trial and error fashion in conventional approaches.

Above this, we also included radiation coefficients dependent on frequency and we could obtain satisfactory results regardless of station azimuth for the whole target frequency band.

This shows the importance of inclusion of frequency dependent radiation coefficients to simulate strong ground motion regardless of station azimuth.

We could get satisfactory matching between synthetic Fourier amplitude spectra and observed Fourier amplitude spectra. This stems from the use of accurate site amplification data extracted by Kawase and Matsuo (2004a, b). We conclude that the accurate estimation of site amplification effects is essential to simulate strong ground motion precisely.

REFERENCES

Asano, K. and T. Iwata (2006). Source process and near-source ground motions of the 2005 West Off Fukuoka Prefecture earthquake, *Earth Planets Space*, **58**, 93-98

Beresnev, I. A. and G. M. Atkinson (1998a). FINSIM–a FORTRAN Program for Simulating Stochastic Acceleration Time Histories from Finite Faults, *Seism. Res. Let.* **69**, 27–32

Beresnev, I. A. and G. M. Atkinson (1998b). Stochastic Finite-Fault Modeling of Ground Motions from the 1994 Northridge, California, Earthquake, *Bull. Seism. Soc. Am.*, **88**, 1392-1401

Boatwright, J. (1988): The seismic radiation from composite models of faulting, *Bull, Seism. Soc. Am.*, **78**, 489-508

Horikawa, H. (2006). Rupture process of the 2005 West Off Fukuoka Prefecture, Japan, earthquake, *Earth Planets Space*, **58**:1, 87-92

Irikura, K., H. Miyake, T. Iwata, K. Kamae, H. Kawabe, and L. A. Dalguer (2004). Recipe For Predicting Strong Ground Motion From Future Large Earthquake, *Proc. 13th World Conf. Earthq. Eng.*, Vancouver, B.C., Canada, 1371 (CD-ROM).

Kagawa, T. (2004) Developing a stochastic Green's function method having more accuracy in long period range to be used in the hybrid method. *J Jpn Assoc Earthqu Eng* **4**:21–32 (in Japanese)

Kawase, H. and Matsuo, H. (2004) Separation of Source, Path, and Site Effects based on the Observed Data by K-NET, KiK-net, and JMA Strong Motion Network, *J. of Str. and Cons. Eng.* (transactions of AIJ) **4**:1, 126-14.

Kawase, H. and Matsuo, H. (2004b). Relationship of S-wave Velocity Structures and Site Effects Separated from the Observed Strong Motion Data of K-NET, KiK-net, and JMA Network, *J. of Str. and Cons. Eng.* (transactions of AIJ) **4**:4, 126-145

Kobayasi R., Miyazaki S and Koketsu, K. (2006) Source processes of the 2005 West Off Fukuoka Prefecture earthquake and its largest aftershock inferred from strong motion and 1-Hz GPS data. *Earth, Planets and Space* 58:1, 57-62

D. Motazedian, G. M. Atkinson (2005). Stochastic Finite-Fault Modeling Based on a Dynamic Corner Frequency, *Bull. Seism. Soc. Am.*, **95**, 995-1010

Somerville, P., K. Irikura, R. Graves, S. Sawada, D. Wald, N. Abrahamson, Iwasaki, Y., Kagawa, T., N. Smith, and Kowada, A. (1999). Characterizing Crustal Earthquake Slip Models for the Prediction of Strong Ground Motion, *Seism. Res. Lett.*, **70**, 59-80

Takenaka, H. Y. Mamada and H. Futamure (2003). Near-source effect on radiation pattern of high-frequency S waves: strong SH-SV mixing observed from aftershocks of the 1997 Northwestern Kagoshima, Japan, earthquakes, *Phys. Earth. Planet. Int.*, **137**, 31-43

Madariaga, R (1979): On the relation between seismic moment and stress drop in the presence of stress and strength heterogeneity, *J. Geophys. Res.*, **84**, 2243-2250.

Mamada, Y. and Takenaka, H. (2004). Strong attenuation of shear waves in the focal region of the 1997 Northwestern Kagoshima earthqakes, Japan, *Bull. Seism. Soc. Am.*,**94**:2, 464-478.

Takenaka, H., Nakamura, T., Yamamoto, Y., Toyokuni, G. and Kawase, H. (2006). Precise location of the fault plane and the onset of the main rupture of the 2005 West Off Fukuoka Prefecture earthquake, *Earth Planets and Space*, **58**:1, 75-80

The Research Group for Active Faults *of* Japan 1991*:* Active faults in *Japan*-sheet maps and inventories (revised edition). The University of Tokyo Press (in *Japanese* with English abstract).

Uehira, K., Shimizu, H., Kanazawa, T., Miyamachi, H., Shinohara, M., Iio, Y., Okada, T., Takahashi, H., Matsuwo, N., Yamada, T., Nakahigashi, K. and Uchida, K. (2006) Precise aftershock distribution of the 2005 West off Fukuoka Prefecture Earthquake (Mj=7.0) by using dense seismic network in ocean and land area, *Earth Planets Space*, **58**:12, 1605-1610